J Mol Model (2015) 21:63
DOI 10.1007/s00894-015-2617-1

ORIGINAL PAPER

Structural prediction of a novel laminarinase from the psychrophilic *Glaciozyma antarctica* PI12 and its temperature adaptation analysis

Sepideh Parvizpour · Jafar Razmara · Ashraf Fadhil Jomah · Mohd Shahir Shamsir · Rosli Mohd Illias

Received: 15 October 2014 / Accepted: 9 February 2015

Abstract Here, we present a novel psychrophilic β-glucanase from *Glaciozyma antarctica* PI12 yeast that has been structurally modeled and analyzed in detail. To our knowledge, this is the first attempt to model a psychrophilic laminarinase from yeast. Because of the low sequence identity (<40 %), a threading method was applied to predict a 3D structure of the enzyme using the MODELLER9v12 program. The results of a comparative study using other mesophilic, thermophilic, and hyperthermophilic laminarinases indicated several amino acid substitutions on the surface of psychrophilic laminarinase that totally increased the flexibility of its structure for efficient catalytic reactions at low temperatures. Whereas several structural factors in the overall structure can explain the weak thermal stability, this research suggests that the psychrophilic adaptation and catalytic activity at low temperatures were achieved through existence of longer loops and shorter or broken helices and strands, an increase in the number of aromatic and hydrophobic residues, a reduction in the number of hydrogen bonds and salt bridges, a higher total solvent accessible surface area, and an increase in the exposure of the hydrophobic side chains to the solvent. The results of comparative molecular dynamics simulation and principal component analysis confirmed the above strategies adopted by psychrophilic laminarinase to increase its catalytic efficiency and structural flexibility to be active at cold temperature.

S. Parvizpour (✉) · A. F. Jomah · M. S. Shamsir
Bioinformatics Research Group, Faculty of Bioscience and Medical Engineering, Universiti Teknologi Malaysia, Johor, Malaysia
e-mail: se.parvizpour@gmail.com

J. Razmara
Department of Computer Sciences, University of Tabriz, Tabriz, Iran

R. M. Illias
Department of Bioprocess Engineering, Faculty of Chemical Engineering, Universiti Teknologi Malaysia, Johor, Malaysia

Published online: 27 February 2015

Keywords Cold adaptation · Flexibility · Laminarinase · Psychrophile · Structure prediction

Introduction

The wide spectrum of different environments presented by earth's biosphere require a variety of adaptive strategies for organisms to stay alive. Temperature is the key factor that affects the biochemical adaptation of living organisms to their environment. Organisms inhabiting extreme temperatures have been of particular interest because the isolated proteins from these organisms can remain stable and function in these environments. These proteins are often desirable for industrial processes and engineering proteins from organisms living at moderate temperatures. They also provide a unique opportunity for researchers to study relationships between their structural characteristics and biological functions.

Psychrophiles are the most adapted microorganisms for living in very cold environments, such as Polar regions and oceans. Enzymes from psychrophilic organisms have evolved toward a high catalytic activity at low temperatures. The cold activity of these enzymes originates mainly from their highly flexible structure, which optimizes their ability to undergo conformational changes during catalysis at cold temperatures [1]. The enzymes have received increased attention due to their potential use in several biotechnological applications, including industrial processes, food industries, and bioremediation [2].

Laminarinase is generally used to identify β-1,3-glucanases that are widely spread throughout bacteria, archaea, and eukaryotes. It plays essential roles in the degradation of microbial saccharides by hydrolyzing the β-1,3-

linkages of glucans and, therefore, is crucial for nutrient uptake and energy production in these microorganisms. The β-1,3-glucanases play several physiological roles in different microorganisms. The enzymes are involved in the protection of plants against fungal pathogens by hydrolyzing β-1,3-glucan as a major component of cell walls. They also regulate seed germination and dormancy in plant seeds and are important in the defence against seed pathogens [3]. β-1,3-glucanases are implicated in degrading the cell wall in viruses during virus release and are enveloped in the virion particle that is involved in virus entrance [3]. Moreover, endo-β-1,3-glucanases have a metabolic function in bacteria by hydrolyzing internal β-1,3-glucosyl linkages, while endo-β-1,3-1,4-glucanases only hydrolyze internal β-1,4-glucosyl linkages with a link at the O-3 position [3]. Commonly, two possible mechanisms are used by these enzymes to catalyze hydrolysis of the substrate: (a) hydrolyzing the substrate by β-1,3-exo-glucanases (EC 3.2.1.58) by consecutively cleaving glucose residues from the nonreducing end and (b) cleaving β-linkages by β-1,3-endo-glucanases (EC 3.2.1.6 and EC 3.2.1.39) at apparently random sites along the polysaccharide chain and releasing smaller oligosaccharides [4]. β-1,3-endo-glucanases have a more prominent role in the cell wall than β-1,3-exo-glucanases due to their physiological activity.

Sequence similarity analysis indicates that the β-glucanase enzyme exists in families 7, 16, and 17 of glycoside hydrolases (GH) (see the CAZy site on http://www.cazy.org). Different GH families exist for microbial and plant β-glucanases without any sequence or structure similarity. The plant enzymes belong to GH-17 and with $(\beta/\alpha)_8$ TIM-barrel fold, whereas the microbial enzymes are classified as members of GH-16 and adopt a β-sandwich architecture. Despite their structural differences, these two β-glucanases with common substrate specificity and activity are an example of functional convergent evolution [5]. The GH-7 and GH-16 families are members of clan GH-B of the glycosyl hydrolases, as they have similar catalytic sites and have most likely evolved from a common ancestor. Enzymes in these families catalyze the glycosyl hydrolysis reaction in a retaining mechanism, where two consecutive inverting steps result in a net retention of the β-anomeric configuration of the reactive sugar unit [6].

The GH-16 contains β-glucanases from a diverse array of organisms including plants, insects, fungi, crustaceans, and nematodes (http://www.cazy.org) where it consists of β-1,3-exo-glucanases (EC 3.2.1.58) and β-1,3-endo-glucanases (EC 3.2.1.6 and EC 3.2.1.39). At least five subgroups can be detected based on phylogenetic study, substrate specificity, and conserved structural features. These include (i) *k*-carrageenases/1,4-β-galactanases, (ii) agarases/1,4-β-galactanases, (iii) nonspecific 1,3(4)-β-glucanases, (iv) lichenases/1,3-1,4-β-d-glucan endohydrolases, and (v) xyloglucan transglucosylases/hydrolases (XTHs) [7]. The subgroups (i), (ii), and (iii) of GH-16 have a highly conserved motif ($WX_{1-4}E[LIV]D[LIVF]X_{0-1}EX_{1-3}$ [GQ]) consisting of a β-bulge, whereas in the subgroups (iv) and (v), the motif E*X*D*X*E, which is one residue shorter, is in the regular β-strand form. Among the solved 3D crystal structures available for β-glucanases in GH16, several 3D structures of the enzyme belong to nonspecific 1,3(4)-β-glucanases subgroup from *P. chrysosporium* (PDB IDs: 2CL2 [7], 2 W39 [8], 2 W52, 2WNE, 2WLQ [9], and 3ILN [10]). The enzymes are reported to be mesophilic, thermophilic and hyperthermophilic; however, β-glucanase isolation from psychrophilic organisms has not been reported until now.

The rapidly growing number of experimentally identified protein sequences has led researchers to use fast computer-based tools for the sequence analysis, structure prediction, and functional annotation of these biological data. Homology modeling plays a key role in creating 3D-structure models based on sequence similarity between newly isolated genes and genes from homologous enzymes having similar fold and function. Additionally, the recently increasing amount of cold-adapted enzymes and their structural details has provided the ability to analyze and understand their molecular adaptation mechanism. In this paper, the structure of a novel 1,3(4)β-d-glucanase from *G. antarctica* PI12 is modeled. The enzyme belongs to the nonspecific 1,3(4)-β-glucanases subgroup of GH-16. The proposed model of the enzyme is also structurally analyzed and simulated using molecular dynamic simulation. Moreover, to clarify the potential cold-adaptation of 1,3(4)-β-d-glucanase, a comparative study is done between the primary sequence and predicted structure of the enzyme and similar mesophilic and thermophilic β-glucanases. Finally, several analyses are performed providing useful details on the thermolability of this enzyme.

Methods

Sequence retrieval and analysis

The full-length gene of the novel β-glucanase, PLAM, was isolated from the cDNA library of *G. Antarctica* PI12. A total of 3 μg of mRNA was used to construct a cDNA library using the CloneMiner cDNA Library Construction Kit (Invitrogen, USA) as per the manufacturer's protocol. The amino acid sequence of the

isolated gene (429 residues) was analyzed using PSI-BLAST [11] and BLAST-PDB [12]. The conserved domains and possible families of the protein were identified using the SUPER-FAMILY HMM server [13].

Building the 3D-model

To build a 3D-model for the protein sequence, the threading method was used because of the lack of a suitable template for the sequence based on the sequence analysis results. Schonoman et al. [14] demonstrated that the threading methods yield high accurate models in comparison with the comparative modeling when a sequence shows a low percentage of identity (<40%). Therefore, the amino acid sequence was submitted to the library of known folds using PSI-BLAST [11], HHPred [15], mGenThreader [16], and Phyre2 [17] to look for the potential available structural templates based on the threading method. From the output list of each server, the most common model was selected and its sequence alignment was given to the MODELLER9v12 program [18] to build 3D-models. A set of 50 models was generated by the MODELLER9v12 program for each alignment, and the model with the highest GA341 score and/or the lowest DOPE score was selected. The best model from the chosen models was finally selected based on the highest value of TM-score [19] that is calculated by TM-align program. The TM-score is an efficient tool widely used to evaluate the quality of a model because it computes a balance between root mean square deviation (RMSD) and the length of alignment. The constructed 3D-model was evaluated by different tools including VERIFY-3D [20], PROCHECK [21], and ERRAT [22] tools.

Molecular dynamic (MD) simulation

To further obtain insights into the structural nature of the cold stability and psychrophilicity of PLAM, we compared the dynamic behavior of the enzyme relative to mesophilic *P. chrysosporium* (2CL2), thermophilic β-glucanase from *A. nocardiopsis sp*. strain F96 (2HYK), and hyperthermophilic *R. marinus* (3ILN). The constructed PLAM model was subjected to energy minimization by the GROMACS 4.6.3 software package. The corresponding pK_a values were identified according to the specified pH, 7, and the molecular environment. Simulations were run at a higher (363 K) and a lower (285 K) temperatures. The four homologous proteins were first placed into four separate suitably sized simulation cubic boxes and solvated with simple point-charged water molecules. In addition, 4, 15, 9, 5 Na+ counter ions were added to neutralize the negative charge in 3ILN, 2HYK, 2CL2, and PLAM, respectively. The entire system was minimlized using the steepest descent of 400 steps. All simulations were performed at a constant temperature and pressure with a non-bonded cut-off of 1.4 Å. The molecular dynamics simulations were performed for 100 ns at 285 K and 363 K, LINCS was used to constrain the bond length, and the particle mesh Ewald method was employed for the electrostatic interactions. The integration time step was 2 fs, and the neighbor list was updated every fifth step using the grid option with a cut-off distance of 1.4 Å. A periodic boundary condition was used with a constant number of particles in the system, pressure, and temperature simulation criteria (NPT). During the simulation, every 1.0 ps of the actual frame was stored. The stabilized structure was taken from the trajectory of the system to determine the quality of the protein geometry and the structure folding reliability.

Additionally, generalized order parameters were calculated for the N-H bonds of the four proteins. The parameters are used as a measure of the degree of spatial restriction of motion (S^2) (the details are in ref. [23]).

Principal component analysis (PCA) was used to determine the most prominent characteristics of the motions along a simulation trajectory [24]. The analysis has been performed to identify the direction and amplitude of the dominant motions using the Dynatraj v1.5 program [25]. The program generates a porcupine plot representing a graphical summary of the motions during the trajectory. The plot shows a cone for each C_α atom reflecting the direction of its motion, where the length of the cone indicates the motion amplitude and the size of the cone specifies the number of such C_α atoms.

Cold adaptation analysis by structural comparison study

The constructed crystal structure of β-glucanase was analyzed for cold adaptation by a comparative study using a mesophilic β-glucanase from *Phanerochaete chrysosporium* (2CL2), a thermophilic β-glucanase from *Alkaliphilic nocardiopsis sp*. strain F96 (2HYK) and β-glucanase from *Rhodothermus marinus* (3ILN) for structural comparison. The VMD program was used to analyze salt bridges during the simulation from 0 to 100*ns*. The salt bridges have been chosen that remain formed during at least 50 % of the simulation time. Moreover, the number of hydrogen bonds and the accessible surface area were calculated during MD simulation. The Swiss-PdbViewer 4.1.0 [26] was used to calculate electrostatic potential and the graphical representation of the 3D-model was prepared by UCSF CHIMERA software [27].

Table 1 Top three proposed templates by different threading tools. 2CL2 obtained the best score including identity and e-value and was selected as the template for PLAM

Server name	Template	Protein	Fold	Identity	E-value
PSI-BLAST	2CL2	Endo-1,3(4)-beta-glucanase	β-sandwich	38%	4e-52
	2WLQ	Nucleophile-D-disabled lama	β-sandwich	37%	3e-51
	3ATG	Endo-1,3-beta-glucanase	β-sandwich	42%	2e-05
HHPred	2CL2	Endo-1,3(4)-beta-glucanase	β-sandwich	38%	2.1e-70
	3DGT	Endo-1,3-beta-glucanase	β-sandwich	19%	2e-49
	3RQO	Glycosyl hydrolases (Gh) family	β-sandwich	20%	9.4e-49
mGenThreader	2CL2	Endo-1,3(4)-beta-glucanase	β-sandwich	NA*	3e-11
	3ATG	Endo-1,3-beta-glucanase	β-sandwich	NA*	1e-06
	2HYK	Endo-1,3-beta-glucanase	β-sandwich	NA*	1e-06
Phyre2	2CL2	endo-1,3(4)-beta-glucanase	β-sandwich	37%	0
	3ILN	Laminarinase	β-sandwich	22%	0
	2VYO	Endo-1,3-beta-glucanase	β-sandwich	21%	0

**NA* not available

Results

Sequence analysis

The complete sequence of β-glucanase has been deposited in the GenBank database. The sequence analysis revealed that the psychrophilic PLAM protein has a low similarity with all known β-glucanase structures in the PDB database. The consensus of all software in Table 1 shows an efficient match of 53 % similarity and 38 % identity with Endo-1,3(4)-β-glucanase from *Phanerochaete chrysosporium* (2CL2). The search result in PSI-BLAST and SUPERFAMILY HMM library identified the catalytic domain of PLAM as glyco-hydrolase and belongs to the β-sandwich family 16 of glycosyl hydrolase.

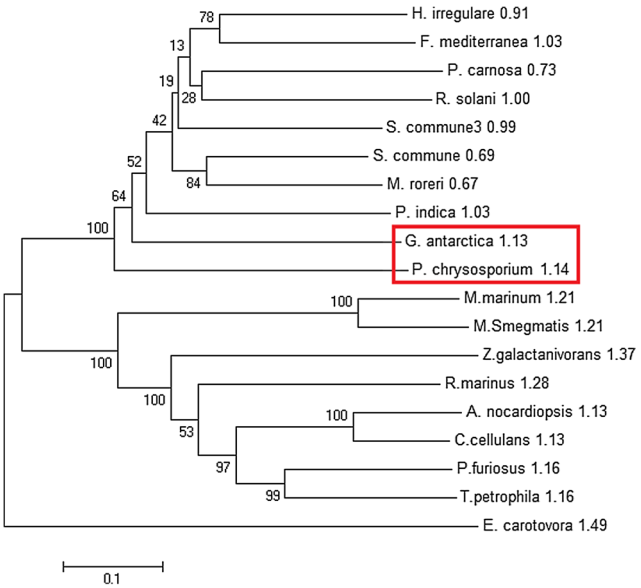

Fig. 1 Phylogenetic tree showing the position of PLAM and other laminarinases from different species

The evolutionary relationship among the psychrophilic PLAM identified in this work and other laminarinases from GH-16 family members was investigated by phylogenetic analysis. The NCBI BlastP service was used to search for complete protein sequence. A set of 22 laminarinase sequences was selected (having an e-value lower than 5×10^{-20}) and aligned using multalin server [28]. The alignment result was used to construct the phylogenetic tree using the maximum likelihood method implemented in the MEGA 5 program [29] and examine the distances among these sequences. Based on the phylogenetic tree in Fig. 1, the closest homologue of PLAM sequence is identified as laminarinase from *P. chrysosporium*.

3D-model prediction

Regarding the sequence analysis results that showed a low percentage of identity for the PLAM protein (38%), we applied the steps from threading method for the purpose of fold recognition. The amino acid sequence of the PLAM protein was submitted to a set of known fold recognition web servers, including PSI-BLAST, HHpred, mGenThreader, and Phyre2. According to the threading results from Table 1, all servers agreed on the catalytic domain of Endo-1,3(4)-β-glucanase from *P. chrysosporium* (2CL2) with the best score, including a high identity and a low e-value. This protein was found to have the same β-sandwich family as PLAM. Based on the sequence alignment results given by

```
Q ss_pred            EEEEEEEECHHHHHCCCCEEEECCCCCCCCCCEEEECHHHHHHCCCEEEECCCEEEEEECC
Q PLAM             2 TGTLRKTHAGPTFFSETDWTFETFADPTHGQVNYVNASVAALNNLVYVNDQNVAILSADM   61 (299)
T c2cl2A_          2 TYHLEDNWVGSAFLS--TFTHEAIADPTHGRVNYVDQATALAKNLTYASGDTLILRADHT   59 (298)
T ss_pred            CEEEEEEECHHHHHH--CCEEECCCCCCCCCCEEECCHHHHCCCCEEEECCEEEEEECCC

Q ss_pred            CCCCCCCCCCEEEEEEECCEEEEEEEEEEEEC-CCCCCCCEEEEEECCCC-CCCCCCEE
Q PLAM            62 GSNLALGQNRNSVRITSKEVYNVGTLVIGDFLR-IPYGCSVWPAFWMFGPN-WPHGGEID  119 (299)
T c2cl2A_         60 TTLSPSGPGRNSVRIRSIKTYTT--HVAVFDVRHMPQGCGTWPAAWETDEGDWPNGGEVD  117 (298)
T ss_pred            CCCCCCCCCEEEEEEEECEEEC--CEEEEEECCCCCCCCEEEEEECCHHHCCCCCCCC

Q ss_pred            EEECCCCCCCEEEEEEECCCCCCCCCCCCEEECCCCCCCCCCCCCCCCCCEEECCHHHHCC
Q PLAM           120 IVEEVNNGEFGNLMSVHSAPGCTRNDSIPMTGGKIGGNCDATDQDWVGCSVRDTSTRSYG  179 (299)
T c2cl2A_        118 IIEGVNDQS-PNAMTLHTGANCAMPASRTMTGHATNNNCDVNTDGNTGCGVQAPTANSYG  176 (298)
T ss_pred            EECCCCCCC-CEEEEEECCCCCCCCCCCCCEEEEECCCCCCCCCCCCCCCCEEECCHHHCC

Q ss_pred            HHHHHCCCEEEEEEECCCCEEEEEECCC--CEEEEEECC--CCCCCCCCCCCCCCCCCCC
Q PLAM           180 PGFVEDQGGVWAMQLATTGVFIWRWPRN--AVPADVTAG--APVPSSWGAPMAAWGSSTC  235 (299)
T c2cl2A_        177 PSFNANGGGWYAMERTNSFIKVWFFPRNAGNVPNDIASGPATINTDNWGTPTAFFPNTNC  236 (298)
T ss_pred            HHHHHCCCEEEEEEECCCEEEEEECCCEEEEECCCCCCCCCCCCCCCCCCCCCCCCCCC

Q ss_pred            CHHHHCCCEEEEEEEECCCCCCCCCCCCCCCCCCCCCHHHCCC-CCCCCCCCEEEEEE
Q PLAM           236 DPAKHFKDLSIVINITTCGDWAGSQYVWQQTTCFAKYPTCAAVVA-DPANFSKAWFEINS  294 (299)
T c2cl2A_        237 DIGSHFDANNIIINLTFCGDWAGQASIFNGAGCP---GSCVDYVNNNPSAFANAYWDIAS  293 (298)
T ss_pred            CHHHHCCCEEEEEEEECCCCCCCCCCCCCCCCCC---CCHHHHCCCCCCCCCCEEEEEE

Q ss_pred            EEEE
Q PLAM           295 VKTY  298 (299)
T c2cl2A_        294 VRVY  297 (298)
T ss_pred            EEEE
```

Fig. 2 The alignment between PLAM and 2CL2 in secondary structure and residue levels predicted by Phyre2 server

different servers, we selected 2CL2 as a suitable template structure for PLAM.

Additionally, the reliability of the constructed model was investigated by a study on the consensus secondary structure of PLAM and 2CL2. Figure 2 shows the alignment between PLAM and 2CL2 in secondary structure and residue level predicted by Phyre2 server. Based on the figure, PLAM and 2CL2 aligned well at all α-helices and β-strands. However, the alignment shows some structural differences in secondary structure level that will be discussed in detail in the model analysis section.

Constructing the 3D-model

Different threading tools were used to build an alignment between PLAM and the endo-1,3(4)-β-glucanase (2CL2) protein that was selected as the 3D-model, and the alignment was submitted to the MODELLER program. The MODELLER program is an efficient tool to automatically calculate and build a model based on an alignment between the query and template sequences. From each alignment tool, a model satisfying the best objective function (the lowest DOPE and/or the highest GA341) was selected and submitted to the TM-align server to evaluate the structural alignment quality based on a TM-score. The score ranges between 0 and 1, whereas a higher score shows a better alignment, and a score more than 0.4 denotes significance. The evaluation results of the models are shown in Table 2.

From the results in Table 2, the model constructed by Phyre2 acquired the best RMSD of 0.42 and TM-score of 0.97. The length of the alignment for this model is slightly longer than the other models; however, this model obtained substantially lower RMSD and higher TM-score than the other models. As a result, we selected the Phyre2 created model as the best model for the PLAM structure. The energy level of the selected model was minimized, and the poor molecular contacts was excluded by GROMACS 4.6.3 software package.

Evaluation of the model

The quality of the created 3D-model was evaluated using several model evaluation web servers. First, the PROCHECK tool was used to assess the backbone conformation based on a Psi/Phi Ramachandran plot. Based on the results, the stereochemical evaluation of backbone psi and Phi dihedral angles of the PLAM revealed that 85.7, 12.3, 1.2, and 0.8 % of residues were falling within the most favored regions, additionally allowed regions, generously allowed regions, and disallowed regions (Ala 270 and Ser 233), respectively. In general, a score (99.6 %) close to 100 % implies good stereo-chemical quality of the model. The results of analysis by VERIFY3D revealed that 97.0 % of the residues had an average 3D-1D score above 0.2, and the remaining residues did not attain this score. For the VERIFY3D score above 80 %, the model quality is considered satisfactory. The overall quality of the model was also assessed by the ERRAT program for nonbonded atomic interactions by comparing the statistics of highly refined structures. The ERRAT score for a

Table 2 Evaluation of the best models created by the MODELLER program for the alignments produced by different servers

Server name	Best model	RMSD	Length of alignment	TM-score
PSI-BLAST	59.pdb	0.45	286	0.96
HHPred	76.pdb	0.47	285	0.94
mGenThreader	18.pdb	0.45	291	0.96
Phyre2	27.pdb	0.42	292	0.97

Table 3 A summary of model evaluations using different tools

Model evaluation tool	Evaluation scheme	Obtained score	Normal range of the score
PROCHECK	The number of residues in the allowed region based on Psi/Phi Ramachandran plot	99.2 %	>90 %
VERIFY3D	The number of residues having an average 3D-1D score above 0.2	97.0 %	>80 %
ERRAT	The overall quality for nonbonded atomic interactions	90.7 %	>50 %

good model is above 50 %, whereas a higher score indicates a better quality [30]. The created model obtained an ERRAT score of 90.73 % that is acceptable in the normal range. A summary of the evaluation results is shown in Table 3. Considering that the PLAM structure was constructed using a threading method with a low sequence identity (less than 40%), the overall scores obtained for the model using different evaluation tools are considered reasonable.

Analysis of the model

The created 3D model of the PLAM protein is shown in Fig. 3. The model has similar structural features to those of other members in family 16 of the glycosyl hydrolases. The PLAM structure consists of an alternating pattern of α-helices and β-strands in its catalytic domain and is considered a β-sandwich fold. The β-sandwich structure has been observed in most of the known microbial glucanase structures and is considered a common folding motif of family 16 laminarinases. The catalytic residues in Fig. 3 are shown as balls and sticks. According to the observation by Krah et al.[31], the PLAM structure consists of two leaflets of antiparallel β-sheets within a complex jelly roll topology, including segmented β-strands, loop connections, and nine small helices. Its secondary structure consists of 30 % β-strands and 12 % α-helices, whereas endo-1,3(4)-beta-glucanase

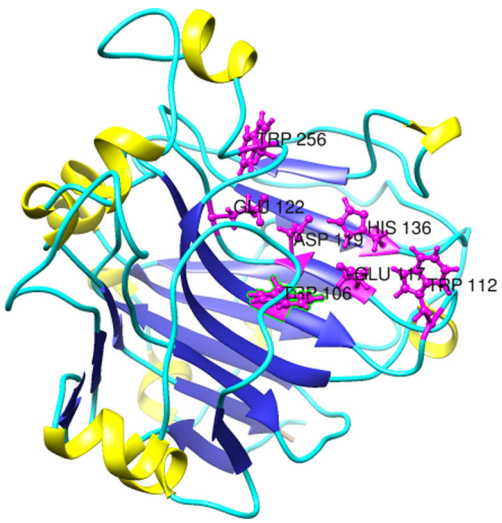

Fig. 3 3D-model of PLAM representing the secondary structure elements

(2CL2) from *P. chrysosporium* as the selected template for the model includes 34 % β-strands and 17 % α-helices.

The PLAM 3D-model was superimposed with 2CL2 as the selected template and is represented in Fig. 4. The superimposition shows an RMSD of 1.2 Å and 68 % coverage of the backbone atoms. Moreover, the conservation of the catalytic domain between PLAM and 2CL2 demonstrates the high accuracy of the constructed 3D-model.

The PLAM protein has an overall structure (Fig. 4) similar to that of the endo-1,3(4)-beta-glucanase enzyme (2CL2) and is not discussed in detail here. However, a visual inspection of their superimposed structure in Fig. 4 indicates two notable differences. First, the PLAM molecule consists of longer external loops on its surface in three different positions (SER16-THR21, GLY109-TRP112, and ALA217-VAL219) instead of two β-sheets (LEU15-HIS20 and THR218-ASN220) and an α-helix (ASP106-ASP109) on the surface of 2CL2 (as shown by red circles in the Fig. 4). Second, most of the long β-sheets on the surface of the 2CL2 molecule are broken into two shorter β-sheets connected by a loop in the PLAM molecule. In addition, the length of β-sheets in the PLAM structure is generally shorter than those of the 2CL2 structure. As a result of longer loops in PLAM structure, Trp256 of PLAM is located on a loop in one of the active sites, whereas it is found on an α-helix in the 2CL2 structure. These key differences around the active sites of PLAM may be responsible for cold adaptation of the molecule by increasing the flexibility of its structure. The possible amplitude of the movement between the secondary structures is increased by longer surface loops and may decrease enzyme stability [32].

Comparative primary sequence analysis

The psychrophilic features of PLAM was examined by a comparative study based on the alignment of its sequence with different laminarinases from mesophilic *P. chrysosporium* (2CL2), thermophilic β-glucanase from *A. nocardiopsis sp*. strain F96 (2HYK), and hyperthermophilic *R. marinus* (PDB code: 3ILN). Based on the multiple sequence alignment results in Fig. 5, the catalytic residues of the examined laminarinases are completely conserved. The previous studies demonstrated that each psychrophilic enzyme has adapted to cold environments by special alterations to its residues. The

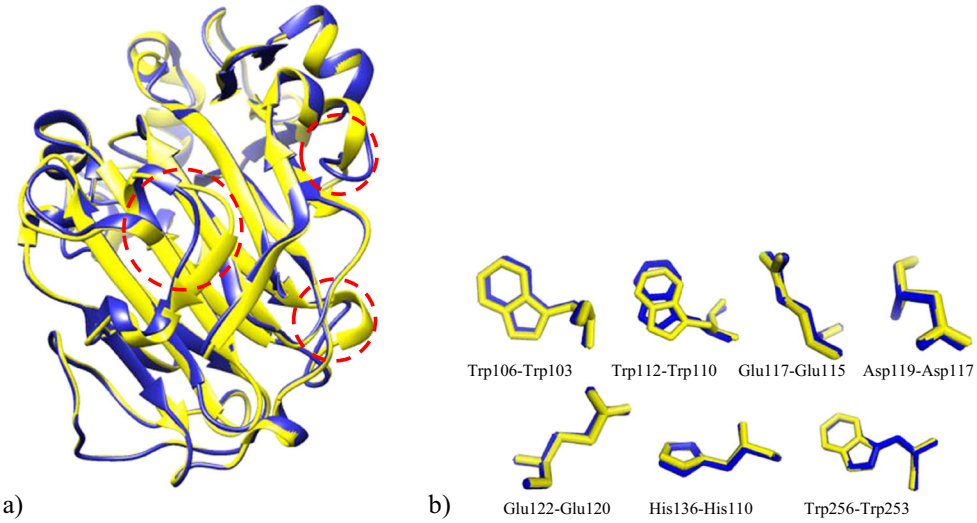

Fig. 4 **a**) Superimposition of PLAM (*blue*) and its template, 2CL2 (*yellow*) in a cartoon representation, **b**) a close up view of the catalytic residue alignment of PLAM and 2CL2

flexibility of a molecule is increased by these alterations, which in turn reduces the stability at certain regions and increases the catalytic efficiency of a protein [33]. Analyzing the multiple sequence alignment of PLAM with other mesophilic, thermophilic, and hyperthermophilic laminarinases in Fig. 5 reveals numerous important replacements in the amino acid residues of psychrophilic and non-psychrophilic proteins. Figure 6 shows these substitutions in the PLAM structure.

Proline is an important substituted amino acid that is closely related to the flexibility of a psychrophilic enzyme. Proline has a covalently linked side chain to the N atom of its backbone that reduces the conformational flexibility of the loop structure by restricting the rotation around the N-C_α bond [34]. Moreover, proline consists of a pyrolidine ring, which restricts the potential conformations of the adjacent residues. Because of the reduction of entropy in the molecular configuration and inhibition of chain flexibility, the stability and local rigidity of the molecule are increased [35]. From the alignment in Fig. 5, it is revealed that proline has been substituted at positions 26, 128, 154, 172, and 207 located on loops of PLAM with other hydrophobic amino acids (alanine, asparagine, aspartate, glutamate). The substitution of these hydrophobic residues in loops plays a key role in increasing the flexibility of PLAM. This substitution also destabilizes the protein structure by constraining the entropy of the water molecule [36]. Additionally, proline substitutions around the loop regions enforce stabilizing effects to generate flexibility on the substrate-binding cleft, which provides the ability to catalyze reactions at cold temperatures [32]. However, the alignment shows several proline residues in PLAM structure (12, 139, 148, 180, and 210) that are conserved with different residues in mesophilic, thermophilic, and hyperthermophilic laminarinases. This

```
      1           $           *                                                                  @             @
PLAM  VTGTLRKTHA GPTFFSETDW TFETFADPTH GQVNYVNASV AALNNLVYVN DQNVAILSAD MGSNLAL... ...GQNRNSV RITSKEVYNV GTLVIGDFLR
2CL2  ATYHLEDNWV GSAFLST..F THEAIADPTH GRVNYVDQAT ALAKNLTYAS GDTLILRADH TTTLSPS... ...GPGRNSV RIRSIKTYTT HVAVF.DVRH
2HYK  ...TESDMRA TLVWSDEFDG PAGSAPDPAN WNHETGDHGW GNNELQNYTD SRANSALDGN GNLVITARQE ADGG..YTSA RLTTQNKVQP QYGRVEASIQ
3ILN  .....RLPHW ELVWSDEFD. .YNGLPDPAK WDYDVGGHGW GNQELQYYTR ARIENARVGG GVLIIEARRE SYEGREYTSA RLVTRGKASW TYGRFEIRAR

      101                 #           # * #$          #                                  *      $
PLAM  IPYGCSVWPA FWM.....F GP.NWPHGGE IDIVEEVNNG EFGNLMSVHS .APGCTRNDS IPMTGGKIGG NCDATDQDWV GCSVRDTSTR SYGPGFVEDQ
2CL2  MPQGCGTWPA AWE.....T DEGDWPNGGE VDIIEGVND. QSPNAMTLHT .GANCAMPAS RTMTGHATNN NCDVNTDGNT GCGVQAPTAN SYGPSFNANG
2HYK  IPRGQGIWPA FWMLG..ADF PNTPWPDSGE IDIMENIGRE PHLVHGSLHG PGY..FGGEP LTGSYMHPQG WSFADTFHTF AVDWRPGSIT WSVDGVAYQT
3ILN  LPSGRGTWPA IWMLPDRQTY GSAYWPDNGE IDIAEHVGFN PDVVHGTVHT KAYNHLLGTQ RGGSIRVPTA RT...DFHVY AIEWTPEEIR WFVDDSLYYR

      201 @               *                                                                  $
PLAM  GGVWAMQLAT TGVFIWRWPR NA..VPADVT AGAPV..PSS WGAPMAAWGS STCDPAKHFK DLSIVINITT CGDWAGSQYV WQQTTCFAKY PTCAAVVADP
2CL2  GGWYAMERTN SFIKVWFFPR NAGNVPNDIA SGPATINTDN WGTPTAFFPN TNCDIGSHFD ANNIIINLTF CGDWAGQASI FNGAGCPGS. .CVDYVNNNP
2HYK  Y.....TSAD TRGNPWVFDQ PFFM..... .......... .......... .......... ....ILNVAV GGDWPGYPDG STQFPQEMRV DYVRVYELG.
3ILN  FPNERLTNPE ADWRHWPFDQ PFHL..... .......... .......... .......... ....IMNIAV GGTWGGQQG. .VDPEAFPAQ LVVDYVRVYR

      301
PLAM  ANFSKAWFEI NSVKTYS
2CL2  SAFANAYWDI ASVRVYQ
2HYK  .......... .......
3ILN  WVE..... .......
```

Fig. 5 Structure-based sequence alignment of laminarinases from *P. chrysosporium* (2CL2) (*green*), *A. nocardiopsis sp.* strain F96 (2HYK) (*blue*), *R. marinus* (3ILN) (*magenta*), and *G. Antarctica* (PLAM) (*yellow*). The catalytic residues are highlighted in *red bold font*

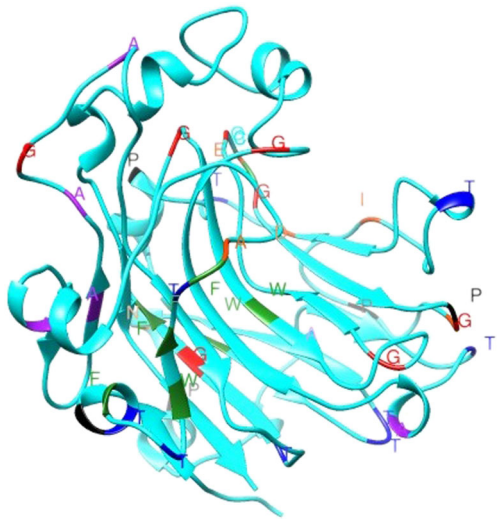

Fig. 6 The amino acids substitution in the PLAM structure. The substitutions are highlighted for glycine (*red*), aromatic residues (*green*), hydrophobic (*magenta*), threonine (*blue*), and proline (*black*) residues

observation supports the idea that the flexibility of different structural components of psychrophilic enzymes has been improved for cold adaptation in the catalytic cycle or other parts of the molecule [34]. In conclusion, the optimal catalysis at low temperatures is achieved by a proper balance between the flexibility and rigidity of a molecule to maintain its 3D conformation in cold environments.

The substitution of aromatic residues in the PLAM sequence is another important change that facilitates the stability of the molecule in appropriate regions. These substitutions can be found at positions 15, 20, 22, 25, 92, 106, 129, and 190 of the PLAM chain, at which the conserved residues in the mesophilic, thermophilic, and hyperthermophilic laminarinases are from non-aromatic residues. The presence of a dipole in aromatic rings allows two favorable interactions, including aromatic-aromatic interactions between aromatic rings at right angles to each other and aromatic-amino interactions between aromatic rings and the side chains of arginine and lysine. Therefore, thermostability is promoted by these interactions through an enthalpic contribution [32]. In addition, it is revealed from the alignment that psychrophilic proteins consist of more aromatic residues than that of the mesophilic counterpart. This demonstrates that psychrophilic proteins need to preserve their 3D-fold in addition to local structural flexibility [37]. Accordingly, it is demonstrated that psychrophilic enzymes apply different strategies to increase their local and global flexibility.

Glycine is a key amino acid to regulate the entropy of the enzyme by increasing the flexibility of the molecule [38]. It has more conformational freedom to allow chain rotation [39] due to the lack of a side chain. The substitution of glycine in psychrophilic laminarinase has occurred at positions 115, 126, 130, and 140 near to functional motif, at which they are conserved with other residues such as histidine, arginine, and asparagine. It was indicated that the presence of glycine around the catalytic residues is related to an increase in the flexibility of the catalytic region [38]. Thus, substitution of tryptophan, proline, alanine, threonine, methionine, and lysine with glycine at positions 115, 126, and 130 in PLAM may improve the efficiency of the catalytic reactions of the psychrophilic PLAM.

Additionally, from the multiple sequence alignment in Fig. 5, some other residue replacements were found. These include the substitution of large residues by smaller residues such as alanine among the same hydrophobic group at positions 42, 55, 59, 66, 231, 233, and 243 of the PLAM structure, whereas the corresponding residues in mesophilic, thermophilic, and hyperthermophilic counterparts are other hydrophobic residues such as valine, glutamine, serine, arginine, asparagine, and leucine. A previous comparative study by Zuber [40] revealed that hydrophobic residues are substituted based on temperature from the more thermophilic valine, phenylalanine, isoleucine, and leucine to the more mesophilic and psychrophilic alanine and methionine. Alanine also appeared at identical PLAM positions 66, 233, and 243 instead of the charged amino acids glutamine and aspartate (mesophilic, thermophilic, and hyperthermophilic laminarinases). This indicates that the small hydrophobic alanine residue is more relevant in cold-adapted enzymes. In addition, the tyrosine, serine, phenylalanine, alanine, glutamine, and valine that are present in mesophilic, thermophilic, and hyperthermophilic laminarinase are replaced by threonine in PLAM at positions 13, 18, 24, 86, 161, 175, 196, 197, and 234. The previous study confirms this observation that the psychrophilic archaea includes fewer charged residues, and more hydrophobic amino acids such as

Table 4 Amino acid content of PLAM for thermostability-related residues compared to averages of family GH-16 members

Residue type	GH-16	PLAM
Gly	9.56±0.21	9.8
Ala	6.18±0.23	10.5
Ser	6.71±0.23	8.2
Thr	7.20±0.23	9.5
Glu	5.08±0.19	3.7
Lys	4.29±0.21	3.5
Arg	4.23±0.19	3.5

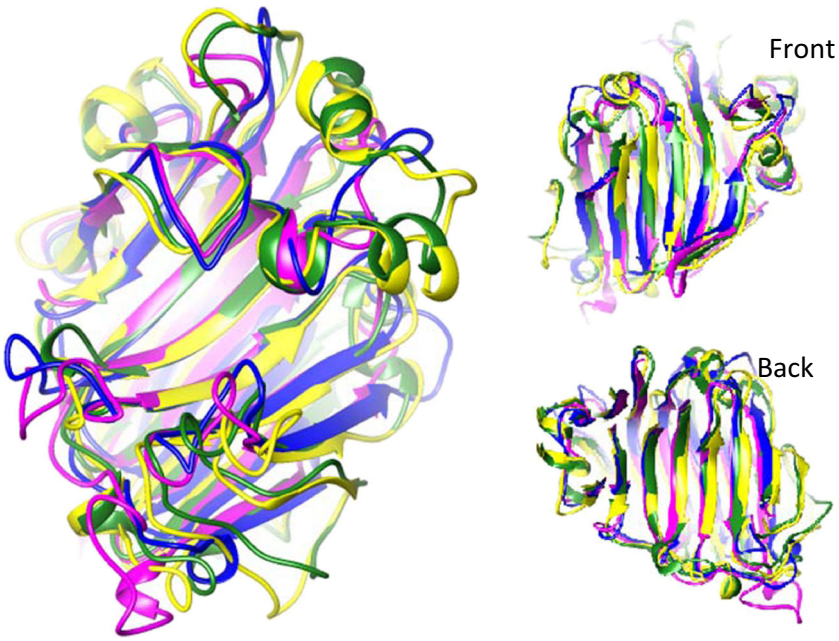

Fig. 7 Structural alignment of laminarinases from *P. chrysosporium* (2CL2) (*green*), *A. nocardiopsis sp*. strain F96 (2HYK) (*blue*), *R. marinus* (3ILN) (*magenta*), and *G. Antarctica* (PLAM) (*yellow*)

alanine, and more noncharged polar residues such as threonine [41].

Additionally, we studied the amino acid content of PLAM relative to other laminarinases from GH-16 family members. Based on the results in Table 4, the sequence of PLAM contains a decreased number of arginine, lysine, phenylalanine, tyrosine, and glutamate residues in comparison with other laminarinases. The decrease of charged and aromatic residues can be correlated to the psychrophilicity of a molecule [42]. The amount of charged amino acids is also correlated with the amount of salt bridges, a key factor for the instability of a protein [43]. In addition, Table 4 shows an increase in the abundance of alanine, glycine, serine, and threonine residues in PLAM relative to other laminarinases in GH-16. This suggests that these residues contribute to making the enzyme structure more flexible and increasing its activity in cold environments.

Molecular dynamic simulation for cold adaptation

The stability of the PLAM structure was analyzed by a non-hierarchical clustering method, called Jarvis-Patrick algorithm [44], which is available through the g_cluster tool in GROMACS. The tool was used to cluster similar conformations in the produced trajectories. The cluster analysis was performed on conformations ensembles generated at 12 °C grouped the matching conformers into three clusters. The central structure of the most populated cluster of the simulation was used as the reference structure in RMSD analysis. The superimposition of the resulting refined structure with the initial PLAM structure revealed that they are approximately identical with a minor RMSD less than 0.1. This high similarity confirms the high quality of the initially created PLAM model.

The dynamic behavior of the PLAM enzyme relative to mesophilic *P. chrysosporium* (2CL2), thermophilic β-laminarinase from *A. nocardiopsis sp*. strain F96 (2HYK), and hyperthermophilic *R. marinus* (3ILN) were compared. Despite the fact that the PLAM sequence has a low identity with three others (<40%) (Fig. 5), the tertiary structures are highly similar. All four structures are essentially identical in the overall fold of the β-sheet leaflets, and the catalytic residues are highly conserved (Fig. 7). However, PLAM has fairly similar loop segments with 2CL2 and differ substantially with 2HYK and 3ILN.

To study the stability and mobility of the four structures, these models were subjected to 100 ns MD simulations at low (12 °C) and high (90 °C) temperatures. The global behavior of the models was analyzed based on the root mean square deviation (RMSD) and the root mean square fluctuations (RMSF) of protein backbone as two crucial parameters for evaluation of the molecules stability during simulation. Regarding the RMSD plot of the proteins in Fig. 8a, PLAM has lower RMSD than three other proteins. Accordingly, the PLAM protein is more stable in this temperature as an optimum temperature for psychrophilic organisms. However, the RMSD of PLAM is higher than the other proteins at 90 °C, and therefore, its stability is low in high

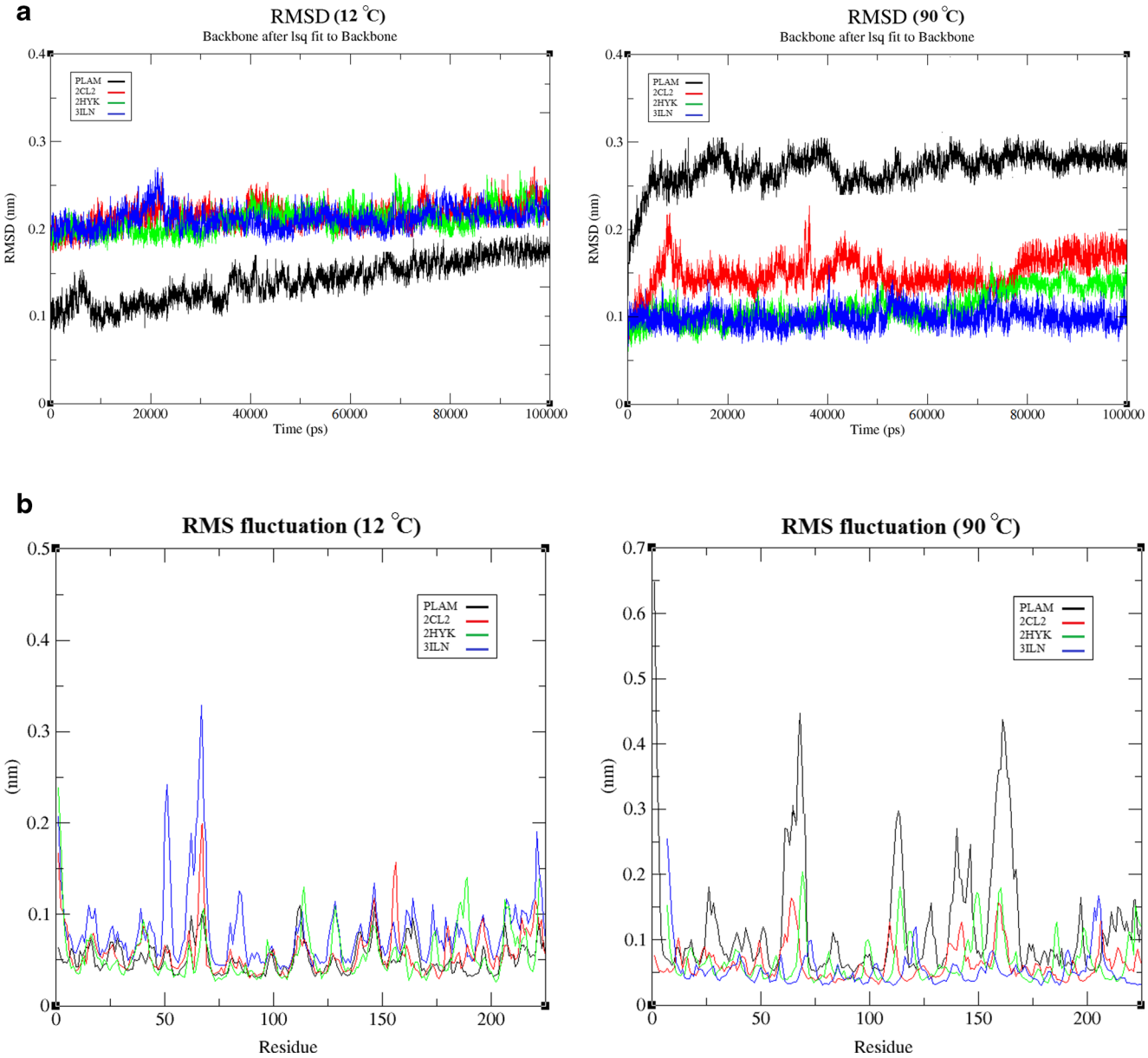

Fig. 8 Dynamic changes of PLAM during MD simulation compared with its homologous proteins, (**a**) RMSD at 12 and 90 °C, and (**b**) RMSF at 12 and 90 °C

temperatures. In addition, the RMSF plot of the proteins as a function of residue number in Fig. 8b shows that the average fluctuation of PLAM residues is relatively low at 12 °C in comparison with three other proteins. However, PLAM generally exhibits a higher average RMSF than the others at 90 °C.

Additionally, flexibility of the above proteins was evaluated and compared using the generalized order parameters (S^2). The order parameters are an interesting descriptor of backbone motion, which characterizes the angular correlation for the dynamics of the N-H bond vector. Their values range from 0 to 1 according to completely isotropic and completely restricted motions, respectively. The results are shown in Fig. 9 as a function of residue numbers. From the results in this figure, the higher flexibility of PLAM structure is confirmed where it has lower value of S^2 than its mesophilic, thermophilic, and hyperthermophilic counterparts.

The principal component analysis (PCA) was used to analyze the first prominent characteristic motions (PC1) along the simulation at 12 °C. Figure 10 shows the porcupine plot of the first eigenvector for 2CL2, 2HYK, 3ILN, and PLAM proteins. According to the porcupine plots of the proteins, PLAM structure consists of longer cones than three other proteins demonstrating longer motions of the atoms during simulation. This

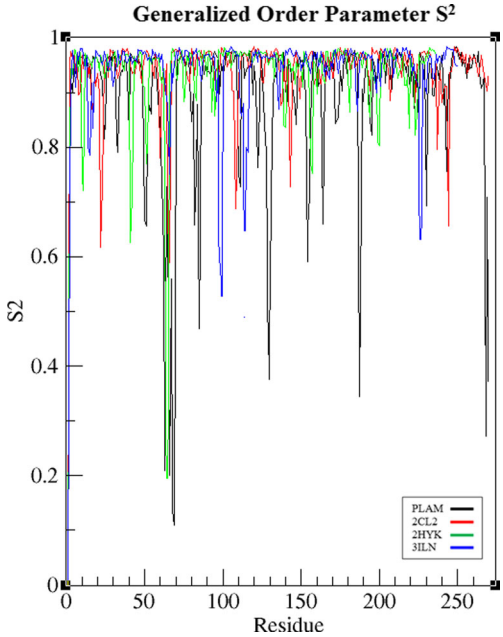

Fig. 9 N-H generalized order parameter S^2 at 12 °C. The order parameters are shown as a function of residue numbers

observation confirms the structural flexibility of psychrophilic PLAM at cold temperature. Additionally, the projection of simulation frames in the 3D-reference subspace formed by the first eigenvectors is represented in

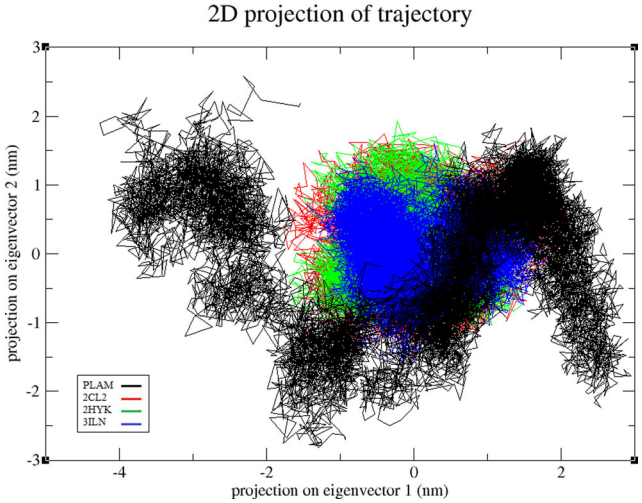

Fig. 11 Projection of simulation frames in the 3D-subspace formed by the first eigenvectors for 2CL2, 2HYK, 3ILN, and PLAM proteins

Fig. 11. The figure confirms and clarifies the above results obtained from PCA analysis, where PLAM achieved a wide sampling of the conformational space in simulation.

Based on the measured structural parameters in MD simulation shown in Table 5, the global folds are mostly preserved in all four structures in the time-scale of the simulation at both temperatures. However, there are

Fig. 10 Dominant motions simulation at 12 °C using principal component analysis. Porcupine plot of the first eigenvector is shown for 2CL2, 2HYK, 3ILN, and PLAM proteins

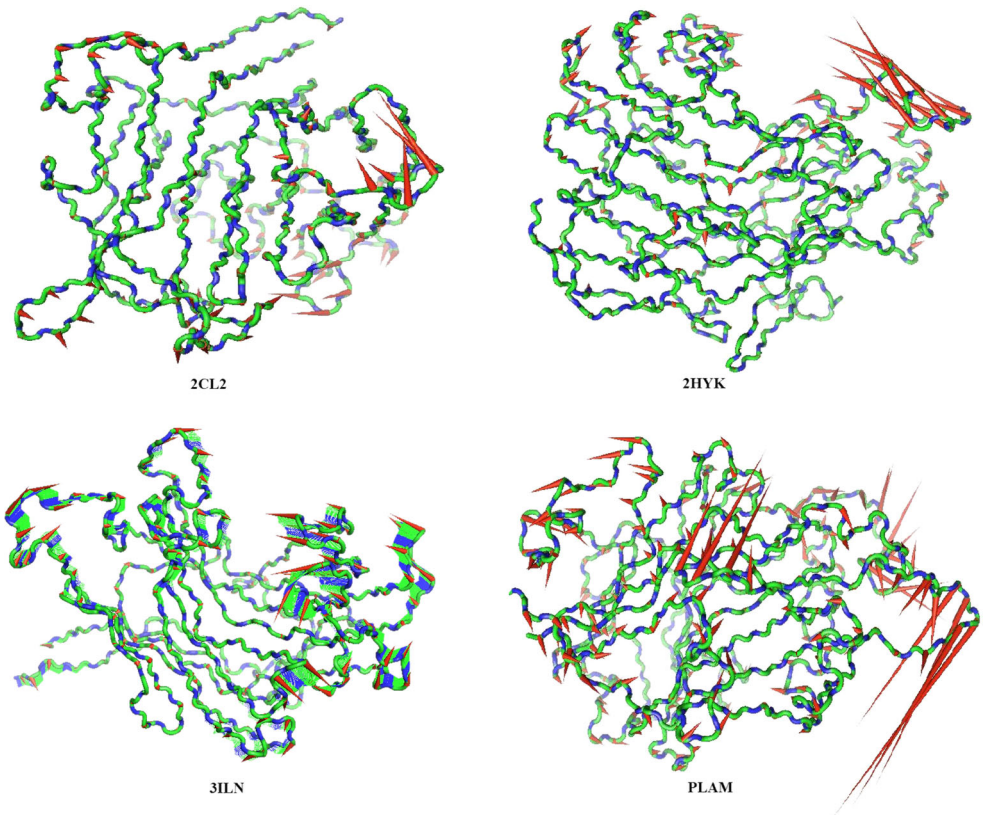

Table 5 Data computed from MD simulation of the homologous laminarinases (*P. chrysosporium* (2CL2), *A. nocardiopsis sp.* strain F96 (2HYK), *R. marinus* (3ILN), and *G. Antarctica* (PLAM)) at 12 °C and 90°C[a]

	PLAM			2CL2			2HYK			3ILN		
	Static structure	12 °C	90 °C	Static structure	12 °C	90 °C	StaticStructure	12 °C	90 °C	Static structure	12 °C	90 °C
R_g (Å)	18.3	18.50.1	18.4±0.1	17.86	18.3±0.1	18.4±0.1	16.46	16.7±0.1	16.8±0.1	17.46	17.9±0.1	17.8±0.1
Sec. struc	41 %	58 %	55 %	54 %	60 %	57 %	44 %	67 %	65 %	50 %	67 %	67 %
HB	192	204±6	190±7	201	214±6	201±7	158	185±5	181±5	178	213±6	200±6
HB per residue[b]	0.64	0.68	0.63	0.66	0.71	0.67	0.63	0.75	0.73	0.70	0.84	0.79
SB	5	7	7	9	10	10	7	11	11	18	25	24
SASA	159.8	150.8±2	148.1±2	178.9	128.9±1	130.8±2	120.0	111.5±1	114.3±1	125.4	122.5±1	122.7±1
HA	61.1	55.7±1	55.9±1	44.9	41.7±1	43.7±1	44.1	40.0±1	41.3±1	48.4	41.2±1	41.6±1

[a] Structural parameters are radius of gyration (R_g), content of secondary structure (Sec. Struc.), number of hydrogen bonds (HB), average number of salt bridges (SB), total solvent accessible surface area (SASA), and number of hydrophobic accessibility (HA). Error bars were computed from the standard deviations obtained from the set of independent simulations for each system. [b] PLAM, 2CL2, 2HYK, and 3ILN have 299, 298, 245, and 251 residues, respectively

some interesting differences between PLAM and three others. For example, the range of gyration of the macromolecules is mostly similar and invariant when the temperature is increased from 12 °C to 90 °C. R_g of PLAM and 2CL2 is slightly larger than two others, but they are commonly temperature independent. Additionally, the secondary structure of all molecules is mostly preserved with increasing temperature. However, the PLAM secondary structure consists of lower percentage than three other laminarinases. This difference was previously discussed in the model analysis section in which psychrophilic PLAM has shorter β-sheets relative to its template model. Another experiment was also done to confirm the existence of longer loops in the PLAM structure (Fig. 4a) and their preservation during MD simulation. Figure 12 shows the secondary structure plot of the PLAM structure using do_dssp tool of Gromacs software for three longer loop locations (SER16-THR21, GLY109-TRP112, and ALA217-VAL219) as discussed in the model analysis section. The plot indicates that PLAM preserves its predicted secondary structure including longer loops on its molecular surface.

The differences between stability of the enzymes at the side-chain level are noticeable. The average number of hydrogen bonds (HB) decreases from 12 °C to 90 °C for all structures. The salt bridges (SB) of all structures are preserved intact when the temperature is increased from 12 °C to 90 °C. The abundance of salt bridges in the PLAM structure is lower than that of its mesophilic, thermophilic, and hyperthermophilic counterparts, thus reinforcing their possible role in PLAM activity at cold temperature. Regarding the longer length of PLAM (298 residue) relative to three other laminarinases, the role of this low number of salt bridges in its structural destabilization is highly indicated. Importantly, both the average number of hydrophobic accessibility (HA) and the total solvent accessibility (SASA) of PLAM are significantly higher than three others. However, there are no meaningful changes for all structures when the temperature is increased. Taking into account that PLAM has a longer sequence than its homologues (PLAM, 2CL2, 2HYK, and 3ILN have 299, 298, 245, 251 residues, respectively), the content of hydrogen bonds per residue is lower in PLAM. In summary, according to the above results, the psychrophilic PLAM exhibits a substantially lower number of SBs and HBs, and a higher number of HA and SASA in comparison with its structural homologues.

In addition to the structural parameters in MD simulation, Table 5 shows the geometrical properties of the four proteins for their static structure. The values obtained for the static structures confirm the results of

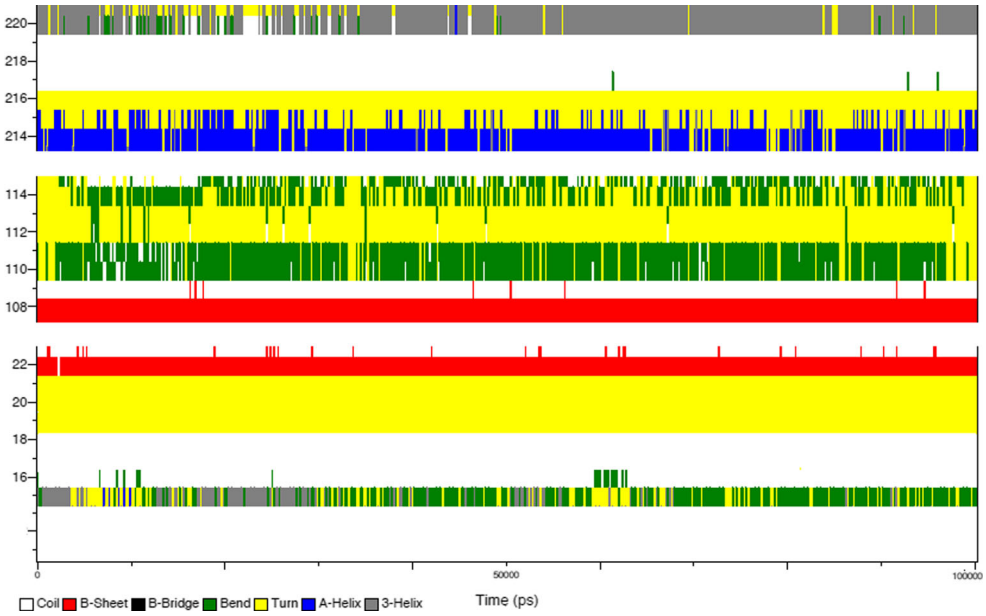

Fig. 12 Secondary structure plot of PLAM during MD simulation for three longer loop locations (SER16-THR21, GLY109-TRP112, and ALA217-VAL219) using DSSP tool of Gromacs software

MD simulation; however, there are some differences between the static and dynamic parameters. For instance, the numbers of salt bridges and hydrogen bonds for static structures are commonly lower than those of MD simulation. Moreover, total solvent accessible surface area (SASA) is decreased for all static structures during MD simulation. These differences are normal due to exhibiting lots of thermal fluctuations caused by temperature and interactions with the solvent during simulation.

Additionally, a comparative study has been done on PLAM structure to investigate its behavior at three cold temperatures using MD simulation. Table 6 shows the simulation results at 4 °C, 12 °C and 18 °C temperatures. The results indicate that PLAM generally preserves its structural behavior at these cold temperatures. This observation is expected for the psychrophilic PLAM, where it is active in these range of temperatures.

Table 6 Data computed from MD simulation of laminarinase from *G. Antarctica* (PLAM)) at 4 °C, 12 °C, and 18 °C

	4 °C	12 °C	18 °C
R_g (Å)	18.9±0.1	18.5±0.1	18.5±0.1
Sec. struc	53%	58%	57%
HB	205±7	204±6	204±6
HB per residue[b]	0.68	0.68	0.68
SB	7	7	7
SASA	149.6±2	150.8±2	149.7±2
HA	55.6±1	55.7±1	55.6±1

Conclusion

The prediction and analysis of a 3D model for β-glucanase PLAM revealed several novel and interesting characteristics of this cold adapted laminarinase from the psychrophilic yeast *G. Antarctica* PI12. The presence of longer loops instead of secondary structural elements and substitution of amino acid residues contribute in the general and local flexibility of the PLAM structure and increase the capability of the enzyme to be active in cold temperatures. The presented findings in this paper will assist future attempts in the rational design of enzymes with enhanced enzymatic capabilities.

References

1. Feller G (2013) Psychrophilic enzymes: from folding to function and biotechnology. Scientifica 2013:1–28
2. Parvizpour S, Razmara J, Ramli ANM, Rosli MI, Shamsir MS (2014) Structural and functional analysis of a novel psychrophilic β-mannanase from Glaciozyma Antarctica PI12. J Comput-aided Molec Des doi: 10.1007/s10822-014-9751-1
3. Ilari A, Fiorillo A, Angelaccio S, Florio R, Chiaraluce R, van der Oost J, Consalvi V (2009) Crystal structure of a family 16 endoglucanase from the hyperthermophile Pyrococcus furiosus–structural basis of substrate recognition. FEBS J 276(4):1048–1058
4. Ahmed R, Jain SK, Shukla PK (2013) modeling and docking studies. Bioinformation 9(16):802–807
5. G. Fibriansah, S. Masuda, N. Koizumi, S. Nakamura, and T. Kumasaka, "The 1.3 A° crystal structure of a novel endo-β-1,3-glucanase of glycoside hydrolase family 16 from alkaliphilic Nocardiopsis sp. strain F96," Proteins: Structure, Function, Bioinformatics, no. April, pp. 683–690, 2007

6. M. L. Sinnott, "Catalytic mechanisms of enzymic glycosyl transfer," chemical reviews, vol. 90, pp. 1171–1202, 1990
7. Vasur J, Kawai R, Larsson AM, Igarashi K, Sandgren M, Samejima M, Ståhlberg J (2006) X-ray crystallographic native sulfur SAD structure determination of laminarinase Lam16A lkr n b Phanerochaete chrysosporium. Acta Crystallogr D Biol Crystallogr 62(Pt 11):1422–1429
8. Vasur J, Kawai R, Andersson E, Igarashi K, Sandgren M, Samejima M, Ståhlberg J (2009) X-ray crystal structures of Phanerochaete chrysosporium Laminarinase 16A in complex with products from lichenin and laminarin hydrolysis. FEBS J 276(14):3858–3869
9. Vasur J, Kawai R, Jonsson KHM, Widmalm G, Engström A, Frank M, Andersson E, Hansson H, Forsberg Z, Igarashi K, Samejima M, Sandgren M, Ståhlberg J (2010) Synthesis of cyclic beta-glucan using laminarinase 16A glycosynthase mutant from the basidiomycete Phanerochaete chrysosporium. J Am Chem Soc 132(5):1724–1730
10. Bleicher L, Prates ET, Gomes TCF, Silveira RL, Nascimento AS, Rojas AL, Golubev A, Martínez L, Skaf MS, Polikarpov I (2011) Molecular basis of the thermostability and thermophilicity of laminarinases: X-ray structure of the hyperthermostable laminarinase from Rhodothermus marinus and molecular dynamics simulations. J Phys Chem B 115(24):7940–7949
11. Altschul SF, Madden TL, Schaffer AA, Zhang J, Zhang Z, Miller W, Lipman DJ (1997) Gapped BLAST and PSI-BLAST: a new generation of protein database search programs. Nucleic Acid Res 25(17):3389–3402
12. Altschul SF, Gish W, Miller W, Myers EW, Lipman DJ (1990) Basic local alignment search tool. J Mol Biol 215:403–410
13. Gough J, Karplus K, Hughey R, Chothia C (2001) Assignment of homology to genome sequences using a library of hidden Markov models that represent all proteins of known structure. J Mol Biol 313(4):903–919
14. Schoonman MJL, Knegtel RMA, Grootenhuis PDJ (1998) Practical evaluation of comparative modelling and threading methods. Comput Chem 22(5):369–375
15. Söding J, Biegert A, Lupas AN (2005) The HHpred interactive server for protein homology detection and structure prediction. Nucleic Acid Res 33(2):W244–W248
16. Jones DT (1999) An efficient and reliable protein fold recognition method for genomic sequences. J Mol Biol 287(4):797–815
17. Kelley LA, Sternberg MJE (2009) Protein structure prediction on the web: a case study using the Phyre server. Nat Protoc 4(3):363–371
18. Eswar N, Webb B, Marti-Renom M, Madhusudhan MS, Eramian D, Shen M-Y, Pieper U, Sali A (2007) Comparative protein structure modeling using MODELLER. Curr Protoc Bioinform 2(1):1–30
19. Zhang Y, Skolnick J (2005) TM-align: a protein structure alignment algorithm based on the TM-score. Nucleic Acid Res 33(7):2302–2309
20. Luthy R, Bowie JU, Eisenberg D (1992) Assessment of protein models with three-dimensional profiles. Nature 356(6364):83–85
21. Laskowski RA, MacArthur MW, Moss DS, Thornton JM (1993) PROCHECK: a program to check the stereochemical quality of protein structures. J Appl Crystallogr 26(2):283–291
22. Colovos C, Yeates TO (1993) Verification of protein structures: patterns of nonbonded atomic interactions. Protein Sci 2(9):1511–1519
23. Papaleo E, Pasi M, Riccardi L, Sambi I, Fantucci P, De Gioia L (2008) Protein flexibility in psychrophilic and mesophilic trypsins. evidence of evolutionary conservation of protein dynamics in trypsin-like serine-proteases. FEBS Lett 582(6):1008–1018
24. Yang LW, Eya E, Bahar I, Kitao A (2009) Principal component analysis of native ensembles of biomolecular structures (PCA_NEST): insights into functional dynamics. Bioinformatics 25:606–614
25. CP B, BA H, ME N (2004) Dynamite: a simple way to gain insight into protein motions. Acta Crystallogr D Biol Crystallogr 60:2280–2287
26. Guex N, Peitsch M (1997) SWISS-MODEL and the Swiss-Pdb viewer: an environment for comparative protein modeling. Electrophoresis 18:2714–2723
27. Pettersen E, Goddard T, Huang C, Couch G, Greenblatt D, Meng E, Ferrin T (2004) UCSF Chimera–a visualization system for exploratory research and analysis. J Comput Chem 25(13):1605–1612
28. Corpet F (1988) Multiple sequence alignment with hierarchical clustering. Nucleic Acids Res 16(22):10881–10890
29. Tamura K, Peterson D, Peterson N, Stecher G, Nei M, Kumar S (2011) MEGA5. molecular evolutionary genetics analysis using maximum likelihood, evolutionary distance, and maximum parsimony methods. Molec Biol Evol 28:2731–2739
30. Chaitanya M, Babajan B, Anuradha C, Naveen M, Rajasekhar C, Madhusudana P, Kumar C (2010) Exploring the molecular basis for selective binding of Mycobacterium tuberculosis Asp kinase toward its natural substrates and feedback inhibitors: a docking and molecular dynamics study. J Mol Model 16(8):1357–1367
31. Krah M, Misselwitz R, Politz O, Thomsen KK, Welfle H, Borriss R (1998) The laminarinase from thermophilic eubacterium Rhodothermus marinus–conformation, stability, and identification of active site carboxylic residues by site-directed mutagenesis. Europ J Biochem / FEBS 257(1):101–111
32. Geralt M, Alimenti C, Vallesi A, Luporini P, Wüthrich K (2013) Thermodynamic stability of psychrophilic and mesophilic pheromones of the protozoan ciliate euplotes. Biology 2(1):142–150
33. Wallon G, Lovett S, Magyar C, Svingor A, Szilagyi A, Zavodszky P, Ringe D, Petsko G (1997) Sequence and homology model of 3-isopropylmalate dehydrogenase from the psychrotrophic bacterium Vibrio sp. I5 suggest reasons for thermal instability. Protein Eng 10(6):665–672
34. Davail S, Feller G, Narinx E, Gerday C (1994) Cold adaptation of proteins. purification, characterization, and sequence of the heatlabile subtilisin from the antarctic psychrophile Bacillus TA41. J Biol Chem 269(26):17448–17453
35. Herning T, Yutani K, Inaka K, Kuroki R, Matsushima M, Kikuchi M (1992) Role of proline residues in human lysozyme stability: a scanning calorimetric study combined with x-ray structure analysis of proline mutants. Biochemistry 31(31):7077–7085
36. Kumar S, Nussinov R (2004) Different roles of electrostatics in heat and in cold: adaptation by citrate synthase. ChemBioChem 5(3):280–290
37. Alimenti C, Vallesi A, Pedrini B, Wu¨thrich K, Luporini P (2009) Molecular cold-adaptation: comparative analysis of two homologous families of psychrophilic and mesophilic signal proteins of the protozoan ciliate, Euplotes. IUBMB Life 61(8):838–845
38. Galkin A, Kulakova L, Ashida H, Sawa Y, Esaki N (1999) Cold adapted alanine dehydrogenases from two Antarctic bacterial strains: gene cloning, protein characterization, and comparison with mesophilic and thermophilic counterparts. Appl Environ Microbiol 65(9):4014–4020
39. Kim SY, Hwang KY, Kim SH, Sung HC, Han YS, Cho Y (1999) Structural basis for cold adaptation. J Biol Chem 274(17):11761–11767
40. Zuber H (1988) Temperature adaptation of lactate dehydrogenase structural, functional and genetic aspects. Biophys Chem 29(1–2): 171–179
41. Saunders N, Thomas T, Curmi P, Mattick J, Kuczek E, Slade R, Davis J, Franzmann P, Boone D, Rusterholtz K, Feldman R, Gates C, Bench S, Sowers K, Kadner K, Aerts A, Dehal P, Detter C, Glavina T, Lucas S, Richardson P, Larimer F, Hauser L, Land M, Cavicchioli R (2003) Mechanisms of thermal adaptation revealed from the genomes of the Antarctic Archaea Methanogenium frigidum and Methanococcoides burtonii. Genome Res 13(7):1241–1255
42. Metpally RPR, Reddy BVB (2009) Comparative proteome analysis of psychrophilic versus mesophilic bacterial species: Insights into the molecular basis of cold adaptation of proteins. BMC Genomics 10:11
43. Kumar S, Nussinov R (2002) Close-range electrostatic interactions in proteins. ChemBioChem 3(7):604–617
44. Jarvis R, Patrick E (1973) Clustering using a similarity measure based on shared near neighbors. IEEE Trans Comput 11:1025–1034